begindocument/before

h_c, η_c and h_c, χ_{c1} production in electron-positron annihilation at B-factories

Monika Narang[1] and Shashank Bhatnagar[2*]
Deptartment of Physics, Chandigarh University, Mohali - 140413, INDIA

Introduction

In this work, we have studied the production of ground and excited axial charmonia $(h_c(nP), \eta_c(n'S))$, and $(\chi_{c1}(nP), h_c(n'P))$[1] for $n, n' = 1, 2$ in e^-e^+ annihilation at $\sqrt{s} = 10.6GeV$ in Bethe- Salpeter (BS) framework, which proceeds through the exchange of a virtual photon on lines of our earlier work [2]. We are studying the processes, $e^-e^+ \to \gamma^* \to h_c\eta_c$ and $e^-e^+ \to \gamma^* \to \chi_{c1}h_c$, both involving four leading-order (LO) Feynman diagrams proceeding through colour-singlet channels, one of which is shown in Figure 1. In these diagrams, there exists a gluon exchange between two of the quark lines, with the photon-quark-antiquark vertex denoted as $ie_Q\gamma_\mu$.

Double Charmonium Production

For the process, $e^-e^+ \to h_c\eta_c$, P and P' represents the external momentums of h_c (1^{+-}) and η_c (0^{-+}) respectively. As the amplitudes for all diagrams are identical, the total amplitude (M_{fi}) for the process is four times that of the Feynman diagram in Figure 1. For the initial process, $e^-e^+ \to h_c\eta_c$, we can formulate the invariant amplitude M^1_{fi}, using one-loop momentum integral, shown in Figure 1 as follow:

$$\begin{aligned} M^1_{fi} &= (ee_Q g^2)F_{12}[\bar{v}^{(s2)}(\bar{p_2})\gamma_\mu u^{(s1)}(\bar{p_1})] \\ &\quad \frac{-1}{k^2}\int\frac{d^4q}{(2\pi)^4}\int\frac{d^4q'}{(2\pi)^4}Tr[\bar{\Psi}_P(P',q')\gamma_\alpha \\ &\quad \bar{\Psi}_A(P,q)\gamma_\beta S_F(p_3)\gamma_\mu]\frac{\delta_{\alpha\beta}}{k^2}, \end{aligned} \quad (1)$$

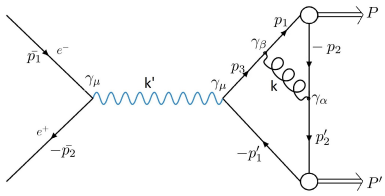

FIG. 1: One of the two leading order Feynmann diagrams contributing to production process.

where, F_{12} is the color factor, defined as $F_{12} = \frac{1}{2}\vec{\lambda_1}.\frac{1}{2}\vec{\lambda_1} = \frac{4}{3}$, $e_Q = \frac{2}{3}e$, and $k = \bar{p_1} + \bar{p_2}$.

The 3-D structures of BS wave-functions, $\Psi_A(\hat{q})$, $\Psi_{A'}(\hat{q})$ and $\Psi_P(\hat{q'})$ (for χ_{c1}, h_c and η_c respectively) are as follows:

$$\begin{aligned} \psi_A(\hat{q}) &= N_A\gamma_5[iM\not{\epsilon} + \not{\epsilon}\not{P} + 2i\frac{\not{\epsilon}\not{P}\not{\hat{q}}}{M}]\phi_A(\hat{q}), \\ \psi_{A'}(\hat{q}) &= N_{A'}\gamma_5(\hat{q}.\epsilon')[M + i\not{P} + \frac{2\not{\hat{q}}\not{P}}{M'}]\phi'_A(\hat{q}) \\ \psi_P(\hat{q}) &= N_P\left[M - i\not{P} + 2\frac{\not{P}\not{\hat{q}}}{m_c}\right]\gamma_5\phi_P(\hat{q}) \end{aligned} \quad (2)$$

where the scalar functions $\phi_A(\hat{q})$, $\phi'_A(\hat{q})$ and $\phi_P(\hat{q'})$ are determined as analytical solutions to the mass spectral equations for $\chi_{c1}(1^{++})$, $h_c(1^{+-})$ and $\eta_c(0^{-+})$ mesons, as presented in [3]. After completing the trace calculations and integral evaluations, we've obtained the final expression for spin-averaged invariant amplitude modulus squared, denoted as $|M_{fi}|^2$,

*Electronic address: shashank_bhatnagar@yahoo.com

as follows:

$$|\bar{M}_{fi}|^2 = \frac{N_A^2 N_P^2}{s^4(-\frac{s}{2}-\frac{M^2}{2}+\frac{M'^2}{4}+m^2)^2} (\frac{64}{3}ee_Q g^2)^2[\Omega+\Omega'] \quad (3)$$

where

$$[\Omega+\Omega'] = \frac{s^2}{8}\xi_1 \sin^2\theta + \frac{s^2}{8}(1+\cos^2\theta)\xi_2 + \frac{s^{3/2}}{4}\sin\theta\cos\theta\xi_3 + \frac{1}{2}(2m_e^2 - s)(\xi_4) \quad (4)$$

In this context, m_c, and m_e respectively denote charm quark mass, and electron mass. We have also used the formula $k^2 = -\frac{s}{4}$. Here, $\xi_1 = (B_1^2 + B_2^2 - \frac{4}{s}{B_4}^2)$, $\xi_2 = 2B_1B_2$, $\xi_3 = -2(B_1 - B_2)B_4$ and $\xi_4 = (M^2B_1 - M'^2B_2)(B_1 - B_2) - {B_4}^2 + s\, B_1B_2$. And B_1, B_2, etc. are the analytical expressions having the solved integrals.

Process ($e^-e^+ \to$)	BSE-CIA	[4]	[5]	[6]
$h_c(1P)\eta_c(1S)$	0.3265	0.73	0.308	0.20
$h_c(1P)\eta_c(2S)$	1.2137	0.99	0.128	
$h_c(2P)\eta_c(1S)$	1.0111	0.48		
$h_c(2P)\eta_c(2S)$	3.8046	0.65		

TABLE I: Cross sections (in fb) for $e^-e^+ \to h_c(nP)\eta_c(nS)$ $(n = 1, 2)$ from the BSE-CIA calculations and comparison with other models.

Similarly, for the process $e^-e^+ \to \chi_{c1}h_c$, the spin-averaged invariant amplitude modulus squared is as follow:

$$|\bar{M}_{fi}|^2 = \frac{N_A^2 N_P^2}{s^4(-\frac{s}{2}-\frac{M^2}{2}+\frac{M'^2}{4}+m^2)^2} (\frac{64}{3}ee_Q g^2)^2\Big[[TR]+[TR']\Big]$$

where $[TR] + [TR'] = \frac{s^2}{16}\sin^2\theta\ \ k_1 + \frac{s^{3/2}}{4}\sin\theta\cos\theta\ k_2 + \frac{s^2}{16}(1+\cos^2\theta)\ k_3 + \frac{1}{2}(2m_e^2 - s)\ k_4$. Again, the terms k_1, k_2, ... are the analytical expressions constituting the trace terms and integrals. Hence, the total cross-section for both the processes can be calculated as follows:

$$\sigma = \frac{1}{16\pi s^{3/2}}|\vec{P'}|\int d\cos\theta |\bar{M}_{fi}|^2. \quad (5)$$

The calculated cross sections for $e^-e^+ \to h_c(nP)\eta_c(n'S)$ and $e^-e^+ \to \chi_{c1}(nP)h_c(n'P)$, where $n, n' = 1, 2$ along with results of other models[4**?** –6] are presented in Table I and Table II.

Process ($e^-e^+ \to$)	BSE-CIA	[4]	[6]	[5]
$\chi_{c1}(1P)h_c(1P)$	0.1124	1.0	0.096	0.258
$\chi_{c1}(1P)h_c(2P)$	0.2519	1.4		
$\chi_{c1}(2P)h_c(1P)$	0.1497			
$\chi_{c1}(2P)h_c(2P)$	0.4122			

TABLE II: Cross sections (in fb) for $e^-e^+ \to \chi_{c1}(nP)\ h_c(n'P)$ $(n = 1, 2)$ from the BSE-CIA calculations and comparison with other models.

Discussion

It can be seen that our results of cross sections for both the production processes in Tables 1, 2 studied here align reasonably with predictions of NRQCD [5] and Relativistic quark model (RQM) [6], but varies from [4]. The accuracy of theoretical predictions across different models can only be assessed when experimental data becomes accessible. Hence, our predictions for these cross sections could prove valuable in the context of future experiments at B-factories, since h_c, η_c, and χ_{c1}, h_c production might provide opportunities for observing h_c with higher statistics in future. Their plots of cross sections [1] versus $\sqrt{s}$ show σ scaling as $\sim 1/\sqrt{s}$ at high energies.

References

[1] M.Narang, S.Bhatnagar (Communicated 2023).

[2] S.Bhatnagar, T.Aruja, V.Guleria, Intl. J. Theo. Phys. 61,211 (2022).

[3] E.Gebrehana, S.Bhatnagar, H.Negash, Phys. Rev. D100, 054034 (2019).

[4] K.Y.Liu, Z.G.He, K.T.Chao, Phys. Rev. D77, 014002 (2008); hep-ph/0408141 (2008).

[5] E.Braaten, J.Lee, Phys. Rev. D 67(5), 054007(2003).

[6] A.P.Martynenko, A. M. Trunin, Physics of Atomic Nuclei 77(6), 777-785(2014).